A Study of the Electrical Propagation in Purkinje Fibers*

Lucas A. Berg[1][0000−0002−8777−0125], Rodrigo Weber dos Santos[1][0000−0002−0633−1391], and Elizabeth M. Cherry[2]

[1] Federal University of Juiz de Fora, Rua José Lourenço Kelmer, s/n – Campus Universitário, Juiz de Fora, MG 36036-900, Brazil
[2] Rochester Institute of Technology, One Lomb Memorial Drive, Rochester, NY 14623-5603, USA

Abstract. Purkinje fibers are fundamental structures in the process of the electrical stimulation of the heart. To allow the contraction of the ventricle muscle, these fibers need to stimulate the myocardium in a synchronized manner. However, certain changes in the properties of these fibers may provide a desynchronization of the heart rate. This can occur through failures in the propagation of the electrical stimulus due to conduction blocks occurring at the junctions that attach the Purkinje fibers to the ventricle muscle. This condition is considered a risk state for cardiac arrhythmias. The aim of this work is to investigate and analyze which properties may affect the propagation velocity and activation time of the Purkinje fibers, such as cell geometry, conductivity, coupling of the fibers with ventricular tissue and number of bifurcations in the network. In order to reach this goal, several Purkinje networks were generated by varying these parameters to perform a sensibility analysis. For the implementation of the computational model, the monodomain equation was used to describe mathematically the phenomenon and the numerical solution was calculated using the Finite Volume Method. The results of the present work were in accordance with those obtained in the literature: the model was able to reproduce certain behaviors that occur in the propagation velocity and activation time of the Purkinje fibers. In addition, the model was able to reproduce the characteristic delay in propagation that occurs at the Purkinje-muscle junctions.

Keywords: Computational Electrophysiology · Purkinje Fibers · Finite Volume Method.

1 Introduction

Ischaemic heart diseases and strokes are still the main cause of deaths worldwide, counting up to approximately 15.2 million of deaths in 2016 [1]. Within this

* Supported by Coordenação de Aperfeiçoamento de Pessoal de Nível Superior (CAPES), Fundação de Amparo à Pesquisa do Estado de Minas Gerais (FAPEMIG), Conselho Nacional de Desenvolvimento Científico e Tecnológico (CNPq), Universidade Federal de Juiz de Fora (UFJF) and National Science Foundation under grant no. CNS-1446312

ICCS Camera Ready Version 2019
To cite this paper please use the final published version:
DOI: 10.1007/978-3-030-22744-9_6

critical scenario it is expected that the cost in cardiac diseases surpass 1044 billions of dollares by 2030 [2].

Even with the recent advances in the treatment of these diseases, like arrhythmias and ischemias, research in this area is still needed. The whole process that leads to this risk state is not completely understood. There are open questions that needs to be further investigated. In this context, computational models that reproduce the electrophysiology of the heart began to be a valuable tool over the years by providing more knowledge about the complex phenomena that are responsible for causing these diseases. Most of these studies aims to analyze the cardiac conduction system.

The cardiac conduction system is a group of specialized cardiac cells of the heart which sends electrical signals to the muscles, enabling them to contract in order to pump the blood from the ventricles to all parts of the body.

It is mainly composed by the sinoatrial node (SA node), the atrioventricular node (AV node), the bundle of His and the Purkinje fibers. The SA node is the natural pacemaker of the heart, on its normal state, it deliveries stimulus to the system. After the stimulus pass through the AV node and the bundle of His, the signal reaches the Purkinje fibers, which are responsible for stimulating the ventricle tissue leading to a contraction of the muscle [3].

Recently, there are several studies that relates problems in the cardiac conduction system and cardiac arrhythmias [4–8]. Furthermore, other studies that mapped the electrical activity of dog and pig hearts, suggest that the Purkinje fibers play an important role in generating ventricular fibrillations at the junctions sites that link the fibers with the ventricular tissue [9–12]. At these juntions, known as Purkinje-muscle junctions (PMJ's), reentry currents could occur, which are a cyclic stimulation that happens over the tissue and is normally triggered by a unidirectional block that occurs at some point of the cardiac conduction system [13].

Also, it was demonstated that the behaviour of the Purkinje system changes when the fibers are couple to a large ventricular mass. There are electrotonic interactions between the fiber and the myocardium which makes the passage of the stimulus from one domain to the another more difficult, leading to delays and even a complete propagation block [14]. These delays normally range from 5 to 15 ms [15] and the main reason for them to happen is a combination of high resistance that the stimulus encounter at the PMJ's together with a low current which unables the ventricular tissue to despolarized. This condition is consider a source-sink mismatch [8, 16].

In this work, it is presented a study which analyzes what factors could affect the electrical stimulus over the Purkinje fibers by evaluating which parameters change the propagation velocity and the activation time of the cells. The main reason for this work is that in previous works the studies only focused in specific features, like the evaluation only of the activation of the PMJ's [17] or by considering how the network geometry affects the activation map [7] or even studying only how the properties of the cells that form the fiber changes the propagation [19].

ICCS Camera Ready Version 2019
To cite this paper please use the final published version:
DOI: 10.1007/978-3-030-22744-9_6

The parameters that were analyzed in the present work were the geometric properties of the cells constituting the fibers, like the diameter and length. Also, the ionic properties were evaluated by using two different cellular models in order to model the dynamics of the Purkinje cells. The first model was proposed by Noble [20], and not only captures the essential features that happens in these cells, but it also provides an opportunity for direct comparison of our results with previous studies. The second model was proposed by Li and Rudy [21] and is a more recent model that is able to capture more complex behaviours, like the calcium cycle.

The implemented model also study the delays that could occur at the PMJ's sites by varying both the electrical resistance and the volume to be stimulated in these regions. Thus, the model was able to reproduce scenarios of conduction block when certain factors were attended.

In addition, the geometry of the Purkinje network could be very irregular, as it was verified in the recent studies from [22]. Because of this, we also consider how the number of bifurcations presented in the network could affect both the propagation velocity and activation time in our simulations.

2 Modeling of the Heart Electrophysiology

The contraction of the cardiac cells is initiated by an electrical activation from an action potential (AP), which is a despolarization current that rises the transmembrane potential of an excitable cell from its resting value, normally between -90 and -80 mV to slightely positive values.

The propagation of the AP from one cell to another can only happen because of gap junctions, which are specialized proteins that enables the flux of ions between neighboring cells as represented by Figure 1.

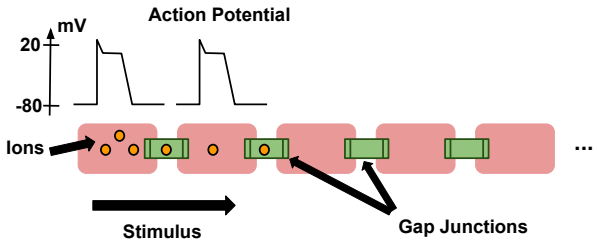

Fig. 1. Representation of the electrical propagation through a Purkinje fiber. The difference in ionic concentration of the cell membrane generates a difference in the potential, which is responsible for triggering an AP, despolarizing the cell when it reaches a certain threashold. In addition, ions can pass from one cell to another by gap junctions, activating the adjacent cells in a wave-like form.

ICCS Camera Ready Version 2019
To cite this paper please use the final published version:
DOI: 10.1007/978-3-030-22744-9_6

2.1 Monodomain model

In order to mathematically reproduce the electrical propagation over the Purkinje fibers we use the unidimensional monodomain model, which is a reaction-diffusion equation.

$$\sigma_x \frac{\partial^2 V_m}{\partial x^2} = \beta \left(C_m \frac{\partial V_m}{\partial t} + I_{ion} + I_{stim} \right), \tag{1}$$

where V_m is the transmembrane potential of the cell given in mV, σ_x is the conductivity from the cells given in mS/cm, β is the surface per volume ratio of the cell given in cm^{-1}, C_m is the capacitance of the membrane given in $\mu F/cm^2$, I_{ion} is an ionic current that depends of the cellular model being used, I_{stim} is a stimulus current.

2.2 Propagation Velocity

One important feature of the electrical propagation through the heart is the velocity in which the stimulus travels. There are differences in the propagation velocity between the Purkinje cells and the ventricular ones. The human cardiac Purkinje cells are characterized by a fast propagation velocity, ranging from 2 to 4 m/s [23]. On the other hand, ventricular cells have relative slower velocity with values between 0.3 to 1.0 m/s [24].

The propagation velocity along a Purkinje fiber could be calculated using the cable equation [27] and by considering that the cable is composed by a set of cells with length h and a diameter d.

$$v = \frac{c}{2C_m} \sqrt{\frac{d}{R_m R_c}}, \tag{2}$$

where v is the propagation velocity of the fiber given in cm/ms, R_c is the citoplasmatic resistivity given in $\Omega.cm$, R_m is the membrane resistivity given in $\Omega.cm^2$ and c is a parameter which depends on the cellular model.

Following the work of [17] the propagation velocity is considered to be constant along the fibers. Because of that, given the distance between two points of the network and the velocity that was measured in this region it is possible to calculate the activation time of a particular cell in the network.

2.3 Numerical solution

The numerical solution of the monodomain equation was done by applying the Finite Volume Method (FVM). The main reason for using the FVM was that is a method based on conservative principals, so that dealing with bifurcations would not be a problem. Also, the method can be applied in complex geometries, such as the Purkinje fibers [18].

For the time discretization of the FVM we divided the diffusion part from the reaction one in equation (1) using the Godunov splitting operator [28]. From

ICCS Camera Ready Version 2019
To cite this paper please use the final published version:
DOI: 10.1007/978-3-030-22744-9_6

this, at each timestep we need to solve two distinct problems, a non-linear system of ODE's given by:

$$\begin{cases} \dfrac{\partial V_m}{\partial t} = \dfrac{1}{C_m}[-I_{ion}(V_m, \eta) + I_{stim}], \\ \dfrac{\partial \eta}{\partial t} = f(V_m, \eta), \end{cases} \tag{3}$$

and a parabolic PDE

$$I_v = \beta \left(C_m \frac{\partial V_m}{\partial t} \right) = \nabla \cdot (\sigma_x \nabla V_m) \,. \tag{4}$$

where η represents the set of variables which controls the ionic channels related to the ionic current I_{ion} of the cellular model.

To approximate the time derivative from equation (4) a implicit Euler scheme was used in order to avoid instabilities problems.

$$\frac{\partial V_m}{\partial t} = \frac{V_m^{n+1} - V_m^n}{\Delta t}, \tag{5}$$

where V^n is the transmembrane potential at timestep n and Δt is the size of the time discretization, which is necessary to advance the PDE in time.

For the time discretization of the non-linear system of ODE's, given by equation (3) an explicit Euler scheme was used with the same timestep of the PDE. For the spacial discretization, the diffusive term from equation (4) was approximated using the following flux:

$$J = -\sigma \nabla V, \tag{6}$$

where $J(\mu A/cm^2)$ is the intracelular flux of current density

$$\nabla \cdot J = -I_v, \tag{7}$$

where $I_v(\mu A/cm^3)$ is a volumetric current which corresponds to the left side of equation (4).

In addition, we will consider an unidimensional cable, which is composed by cylinders and will represent the Purkinje cells, as it is illustrated by Figure 2. These will be the control volumes of FVM, in which at the center of each one will be a node containing the amount of interest V_m.

ICCS Camera Ready Version 2019
To cite this paper please use the final published version:
DOI: 10.1007/978-3-030-22744-9_6

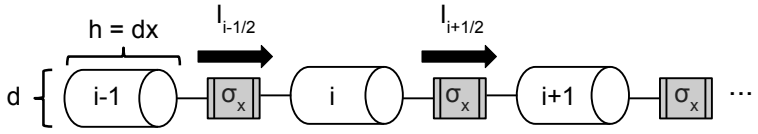

Fig. 2. Space discretization used for modeling the Purkinje fibers. Each Purkinje cell has diameter d and a length h. The length of the cells have the same value of the space discretization size dx. Between the cells, there are current fluxes through the faces of the control volumes.

After that, we define the FVM equations by integrating (7) over an individual control volume V_i with a value equal to $\pi d^2 h/4$.

$$\int_{\Omega} \nabla \cdot J dv = -\int_{\Omega} I_v dv. \tag{8}$$

Then, applying the divergence theorem on (8).

$$\int_{\Omega} \nabla \cdot J dv = \int_{\partial\Omega} J \cdot \boldsymbol{\xi} ds, \tag{9}$$

where $\boldsymbol{\xi}$ is an unitary vector which points to the boundary $\partial\Omega$.

$$\int_{\partial\Omega} J_i \cdot \boldsymbol{\xi} ds = -\int_{\Omega} I_v dv. \tag{10}$$

Finally, assuming that I_v represents a mean value for each particular volume and substituting (4) into (10).

$$\beta C_m \left.\frac{\partial V_m}{\partial t}\right|_i = \frac{-\int_{\partial\Omega} J_i \cdot \boldsymbol{\xi} ds}{\pi . d^2 . h/4}. \tag{11}$$

Calculating J_i for each control volume by dividing the flux into a sum of fluxes over each face and remembering that we have only an input and a output flux at each control volume.

$$\int_{\partial\Omega} J_i \cdot \boldsymbol{\xi} ds = (I_{out} - I_{in}), \tag{12}$$

where the current between two control volumes i and j are calculated as follows

$$I_{i,j} = -\sigma_x \left.\frac{\partial V_m}{\partial x}\right|_{i,j} \frac{\pi . d^2}{4}, \tag{13}$$

where a central finite difference approximation was used for the space derivative on equation (13):

ICCS Camera Ready Version 2019
To cite this paper please use the final published version:
DOI: 10.1007/978-3-030-22744-9_6

$$\left.\frac{\partial V_m}{\partial x}\right|_{i,j} = \frac{V_j - V_i}{h}. \tag{14}$$

In order to model the PMJ's we consider that the last Purkinje cell of the fiber will be linked to a large myocardium cell, which has a volume equivalent to the region to be stimulated over the ventricular tissue. This connection was implemented by adding a discrete resistor R_{PMJ} between the last Purkinje cell and the myocardium cell as shown in Figure 3.

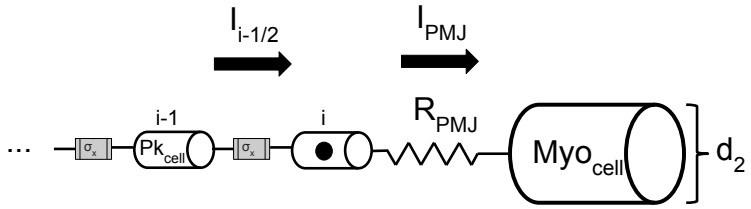

Fig. 3. Space discretization used for modeling the Purkinje-muscle junctions. The myocardium cell has a larger diameter d_2 than the Purkinje cells.

Furthermore, the value of the current I_{PMJ} that passes through the resistor R_{PMJ} is given by

$$I_{PMJ} = \frac{(V_{pk} - V_{myo})}{R_{PMJ}}, \tag{15}$$

where V_{pk} is the tramsmembrane potential from the Purkinje cell and V_{myo} is the transmembrane potential of the myocardium cell.

To be able to analyze the behaviour of the characteristic delay that occur at the PMJ's sites we define a γ parameter, which is the product between the resistance of the PMJ and the volume of the myocardium cell.

$$\gamma = \frac{\pi.d_2^2.h}{4}.R_{PMJ} \tag{16}$$

3 Results and Discussions

3.1 Stimulus protocol and cellular models

For all the experiments of this work we use the following stimulus protocol.

Initially, we perform a simulation so that the system could reach its steady-state, where $\Delta t = 0.01$ ms and a stimulus current I_{stim} is applied in periods of 500 ms in the first 5 cells of the fiber. At the end of this first simulation we save the state of every cell in the network and load this state as the initial condition

ICCS Camera Ready Version 2019
To cite this paper please use the final published version:
DOI: 10.1007/978-3-030-22744-9_6

for a second simulation, in which the propagation velocity and activation times will be calculated. This was done in order to get a more reliable result since the system will be at equilibrium.

Regarding the cellular models for the ionic current I_{ion} that appears on equation (3) we use two models that are specifically for cardiac Purkinje cells, the Noble model [20] and the Li & Rudy model [21].

3.2 Model for the propagation velocity

The first experiment of this work has the objective of calibrating the parameters related to the monodomain model until it reaches the same behaviour of the analitical expression given by (2), which describes the propagation velocity over the fiber.

In order to achieve this the parameter c from equation (2) needs to be calculated based on the cell properties we were using. On [27] there is a table with typical values for the parameters from equation (2) for different types of cells, for this work we use the values related to the cardiac mammal muscle in this table.

Considering some works found in the literature [29–31] an average value for the propagation velocity in a dog Purkinje fiber with a diameter in the range of $d = 35\mu m$ is aproximately 2 to 3.5 m/s. By using the values $R_m = 7k\Omega.cm^2$, $R_c = 150\Omega.cm$, $C_m = 1.2\mu F/cm^2$, $d = 35\mu m$ and $v = 2.6m/s$ on equation (2) we calculate $c = 10.808$. This result will be consider the analitical solution for the model in this experiment.

For the numerical approximation we changed the value of the conductivity σ_x in order to get a propagation velocity close to the one given by the analitical solution. Then, we measured the velocity on a $2cm$ cable composed of Purkinje cells with a diameter and length equal to $d = 35\mu m$ and $dx = 164\mu m$, respectively. After some tests we found the values $\sigma_x = 0.004mS/cm$ for the Noble model and $\sigma_x = 0.0019mS/cm$ for the Li & Rudy model, which resulted in a propagation velocity along the cable equals to $v = 2.645m/s$, which was close to the value from the analitical model.

By varying the value of the diameter d of the Purkinje cells we could them verify how the propagation velocity behaves along the cable. In Figure 4 we measured the propagation velocity in a $2cm$ cable by using an initial diameter of $d = 10\mu m$ and we incremented this value by $5\mu m$ until it reaches $d = 50\mu m$.

ICCS Camera Ready Version 2019
To cite this paper please use the final published version:
DOI: 10.1007/978-3-030-22744-9_6

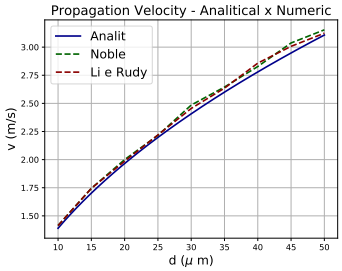

Fig. 4. Comparison between the analitical solution given by (2) and the numerical one. The propagation velocity was calculated for a Purkinje cell set at the middle of the $2cm$ cable.

As can be verify, the results from our numerical model were really close to the analitical one. Furthermore, the behaviour of the propagation velocity was in accordance with the observations found in the literature [30], which says that the velocity along a cable decays with a factor proportional to the $\sqrt{d}$.

3.3 Model with Purkinje-muscle junctions

In the next experiment we explore how the introduction of a PMJ would affect the activation time along the fiber. The simulations were done using again a $2cm$ cable, which will be representing the Purkinje fiber. At the end of the cable a PMJ with resistance $R_{PMJ} = 11000k\Omega$ was added and then linked to a myocardium cell. The characteristic delay was calculated by taking the difference between the activation time of the last Purkinje cell and the myocardium cell.

To analyze the characteristic delay that happens at the PMJ's sites we vary the value of the parameter γ and the diameter d of the Purkinje cells, so that we could study in which condition there will be propagation blocks as can be seen in Figure 5.

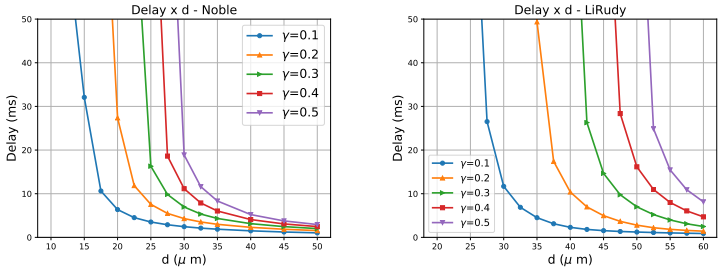

Fig. 5. Comparison between the characteristic delay given in ms and the diameter of the Purkinje cells when the γ parameter changes for both the Noble and Li & Rudy model.

ICCS Camera Ready Version 2019
To cite this paper please use the final published version:
DOI: 10.1007/978-3-030-22744-9_6

As can be visualized in Figure 5, both cellular models obtain similar results. It is important to note that there is a value for the diameter where the characteristic delay begins to assume high values until it leads to a complete block of the stimulus, unabling the myocardium cell to be despolarized, characterized by the sudden peaks in the results. Also, with this simulation we could check that there is a relation between the characteristic delay and the γ parameter. As we increase the value γ the delay time increases proportionally, since a high value of γ means either a large ventricular mass to be stimulated or a high resistance of the PMJ. In both cases we need more current from the fiber in order to trigger an AP at the myocardium cell.

Regarding the diameter of the Purkinje cells the relation between this parameter and the characteristic delay is inversely proportional. The reason is that with a larger diameter more current could travel through the fiber since its transversal area will be wider, which makes the despolarization of the myocardium cell to happen more easily.

3.4 Model with bifurcations

The last experiment of this work studies the effects of bifurcations over the Purkinje fibers. Different types of networks were generated with different levels of bifurcations as shown in Figure 6.

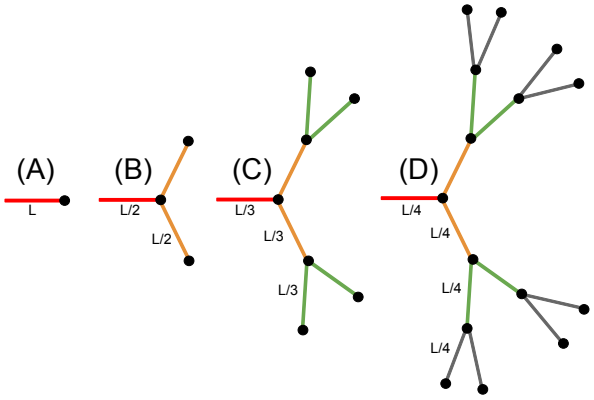

Fig. 6. Networks that were used in the experiments that evaluate the influence of bifurcations over the activation time. Each one of the four networks represents a structure with a different level of bifurcations. The distance between the source of the stimulus and the terminal points of the networks are always equals to L. (A) Level 0. (B) Level 1. (C) Level 2. (D) Level 3.

In addition, we decrease the diameter of the Purkinje cells from one level of the network to another. This decision was made by observing images of Purkinje

ICCS Camera Ready Version 2019
To cite this paper please use the final published version:
DOI: 10.1007/978-3-030-22744-9_6

fibers of a calf [26]. The value of the diameter at a certain level k of the network it now be given by (17).

$$\begin{cases} d_k = d_0, \ if \ k = 0, \\ d_k = \delta.d_{k-1}, \ if \ k \neq 0, \end{cases} \tag{17}$$

where d_k is the diameter of a Purkinje cell at a level k in the network and δ is the ratio in which the diameter is decreased.

The simulations were done using the same two cellular models and by adding a PMJ with $\gamma = 0.2$ at the end of each fiber. For the space discretization we use $dx = 164\mu m$, a initial diameter $d_0 = 30\mu m$ for the Noble model and $d_0 = 55\mu m$ for the Li & Rudy model. The decrease ratio for the diameter was tested within the range $\delta = \{90\%, 80\%, 70\%\}$ and the distance from the source of the stimulus to each terminal was $L = 2$cm.

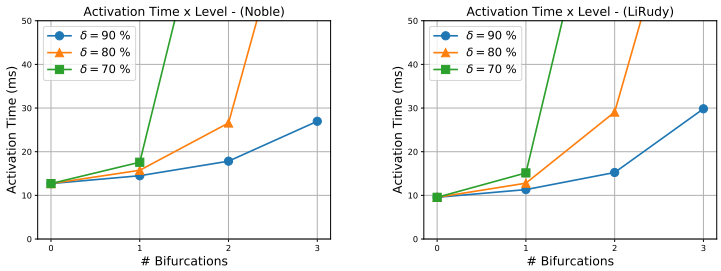

Fig. 7. Results showing the activation time of the myocardium cell considering the number of bifurcations the stimulus had to pass through until it reaches the end of the fiber as the diameter decreases by a ratio δ, for both the Noble and Li & Rudy model.

In Figure 7 it can be verified that in both celullar models the activation time of the myocardium cell increases proportionally to the number of bifurcations. This happens because after a bifurcation the diameter decreases by following equation (17), which makes the activation much harder, since the networks that had more bifurcations will have a smaller diameter at the last level of the fibers.

Based in this observation we perform another experiment that test the effects of also decreasing the myocardium volume to be stimulated by the fibers. Mainly because, the Purkinje fibers seems to be well distributed over the ventricular tissue in order to proper activate the muscles and to reduce propagation blocks [26]. This was done by calculating the value of γ based on how many levels of bifurcation a certain network had.

$$\gamma_k = \frac{\gamma_0}{2^k}, \tag{18}$$

ICCS Camera Ready Version 2019
To cite this paper please use the final published version:
DOI: 10.1007/978-3-030-22744-9_6

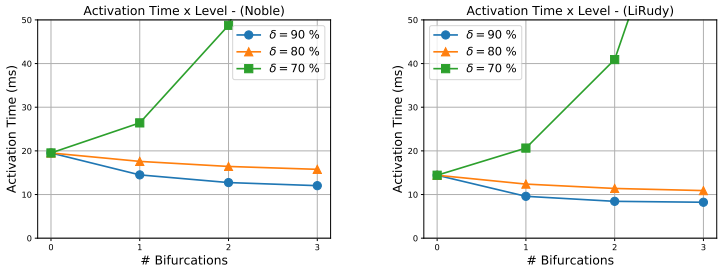

Fig. 8. Results showing the activation time of the myocardium cell considering the decreasing of the parameter γ using (18) as the diameter of cells decreases by a ratio δ.

Analyzing the results from Figure 8 the decreasing of the γ parameter could avoid some of the propagation blocks that happen in the previous test. This behaviour can be justify by the fact that with less resistance at the PMJ sites, the fibers which had a small diameter could now despolarize the myocardium cell.

4 Conclusions

In this work it was studied which features from the Purkinje fibers change the propagation velocity and the activation time within these structures. From the results of the experiments, geometric parameters, like the diameter of the Purkinje cells, were the ones that had the most influence among the others. Meaning that they could play an important role in sustaining arrhythmias.

From the results of the experiments presented in this work we could retrieve some relevant information about the factors that could affect the propagation velocity and the activation over the Purkinje fibers.

In the first experiment, it was possible to validate certain behaviours found in the literature. The implemented model was able to reproduce the proportionality between the diameter of the Purkinje cells and propagation velocity along the fiber, which according to some works is proportional to $\sqrt{d}$ [27, 25]. Thus, both cellular models reproduced the same behaviour as it was expected.

From the results of the second experiment it was shown that Purkinje fibers with a small diameter were not able to stimulate a large region of the myocardium, generating propagation blocks over the PMJ's sites. These blocks mainly occur because there are cells that could not achieve the current threshold necessary to activate the myocardium cell, which is characterized as a source-sink mismatch.

The last experiment fortifies the idea that the activation of the ventricular tissue depends of how well distributed the fibers are over this domain, which is actually observed in nature. The ramifications of the Purkinje network seems to be a way to homogeneously cover the myocardium tissue in order to increase the

ICCS Camera Ready Version 2019
To cite this paper please use the final published version:
DOI: 10.1007/978-3-030-22744-9_6

superficial area of the network and minimize the energetic cost for the stimulation of the ventricles.

Furthermore, the implemented model was able to reproduce the characteristic delay that occurs at the PMJ's sites. The implementation using the Finite Volume Method and the coupling using a resistor linked to a larger control volume has proved to be very effective, since it was able to generate the same results that were observed in the literature.

References

1. World Health Organization.: https://www.who.int. Last accessed 28 Dec 2018.
2. A. H. Association et al.: Heart disease and stroke statistics: 2017 at-a-glance (2017).
3. Clayton, R. H. et al.: Models of cardiac tissue electrophysiology: progress, challenges and open questions. Progress in biophysics and molecular biology **104**(1-3), 22–48 (2011).
4. M. Deo, P. M. Boyle, A. M. Kim, and E. J. Vigmond.: Arrhythmogenesis by single ectopic beats originating in the Purkinje system. American Journal of Physiology-Heart and Circulatory Physiology **299**(4), H1002–H1011 (2010).
5. E. Behradfar, A. Nygren, and E. J. Vigmond.: The role of Purkinje-myocardial coupling during ventricular arrhythmia: a modeling study. PloS one **9**(2), 1–9 (2014).
6. W. Quan and Y. Rudy.: Unidirectional block and reentry of cardiac excitation: a model study. Circulation Research **66**(2), 367–382 (1990).
7. P. M. Boyle, M. Deo, G. Plank, and E. J. Vigmond.: Purkinje-mediated effects in the response of quiescent ventricles to defibrillation shocks. Annals of Biomedical Engineering **38**(2), 456–468 (2010).
8. R. S. Oliveira, S. Alonso, F. O. Campos, B. M. Rocha, J. F. Fernandes, T. Kuehne, R. W. dos Santos.: Ectopic beats arise from micro-reentries near infarct regions in simulations of a patient-specific heart model. Scientific reports **8**(1), 16392 (2018).
9. O. Berenfeld and J. Jalife.: Purkinje-muscle reentry as a mechanism of polymorphic ventricular arrhythmias in a 3-dimensional model of the ventricles. Circulation Research **82**(10), 1063–1077 (1998).
10. J. S. Allison, H. Qin, D. J. Dosdall, J. Huang, J. C. Newton, J. D. Allred, W. M. Smith, and R. E. Ideker.: The transmural activation sequence in porcine and canine left ventricle is markedly different during long-duration ventricular fibrillation. Journal of Cardiovascular Electrophysiology **18**(12), 1306–1312 (2007).
11. P. B. Tabereaux, G. P. Walcott, J. M. Rogers, J. Kim, D. J. Dosdall, P. G. Robertson, C. R. Killingsworth, W. M. Smith, and R. E. Ideker.: Activation patterns of Purkinje fibers during long-duration ventricular fibrillation in an isolated canine heart model. Circulation Research **116**(10), 1113–1119 (2007).
12. L. Li, Q. Jin, J. Huang, K. A. Cheng, and R. E. Ideker.: Intramural foci during long duration fibrillation in the pig ventricle. Circulation Research **102**(10), 1256–1264 (2008).
13. D. C. Sigg, P. A. Iaizzo, Y.-F. Xiao, and B. He.: Cardiac electrophysiology methods and models. Springer Science & Business Media, (2010).
14. R. W. dos Santos, F. O. Campos, L. N. Ciuffo, A. Nygren, W. Giles and H. Koch.: ATXII Effects on the Apparent Location of M Cells in a Computational Model of a Human Left Ventricular Wedge. Journal of cardiovascular electrophysiology **17**, S86–S95 (2006).

ICCS Camera Ready Version 2019
To cite this paper please use the final published version:
DOI: 10.1007/978-3-030-22744-9_6

15. S. Palamara, C. Vergara, E. Faggiano, and F. Nobile.: An effective algorithm for the generation of patient-specific Purkinje networks in computational electrocardiology. Journal of Computational Physics **283**, 495–517 (2015).
16. Y. Xie, D. Sato, A. Garfinkel, Z. Qu, and J. N. Weiss.: So little source, so much sink: requirements for afterdepolarizations to propagate in tissue. Biophysical Journal **99**(5), 1408–1415 (2010).
17. C. Vergara, S. Palamara, D. Catanzariti, C. Pangrazzi, F. Nobile, M. Centonze, E. Faggiano, M. Maines, A. Quarteroni, and G. Vergara.: Patient-specific computational generation of the Purkinje network driven by clinical measuraments. MOX Report (9), (2013).
18. R. S. Oliveira, M. B. Rocha, D. Burgarelli, W. M. Jr, C. Constantinides and R. W. dos Santos.: Performance evaluation of GPU parallelization, space-time adaptive algorithms, and their combination for simulating cardiac electrophysiology. International journal for numerical methods in biomedical engineering **34**(2), e2913 (2018).
19. F. O. Campos, Y. Shiferaw, A. J. Prassl, P. M. Boyle, E. J. Vigmond, and G. Plank.: Stochastic spontaneous calcium release events trigger premature ventricular complexes by overcoming electrotonic load. Cardiovascular Research **107**(1), 175–183 (2015).
20. D. Noble.: A modification of the HodgkinHuxley equations applicable to Purkinje fibre action and pacemaker potentials. The Journal of Physiology **160**(2), 317–352 (1962).
21. P. Li and Y. Rudy.: A model of canine Purkinje cell electrophysiology and Ca2+ cycling. Circulation Research, CIRCRESAHA–111 (2011).
22. D. Duan, S. Yu, Y. Cui, and C. Li.: Morphological study of the atrioventricular conduction system and Purkinje fibers in yak. Journal of Morphology **278**(7), 975–986 (2017).
23. P. F. Carnefield, A. L. Wit, and B. F. Hoffman.: Conduction of the cardiac impulse: III. Characteristics of very slow conduction. The Journal of General Physiology **59**(2), 227–246 (1972).
24. D. Bers.: Excitation-contraction coupling and cardiac contractile force. Springer Science & Business Media, (2001).
25. N. Sperelakis.: Cell physiology source book: essentials of membrane biophysics. Elsevier, (2012).
26. R. Sebastian, V. Zimmerman, D. Romero, D. Sanchez-Quintana and A. F. Frangi.: Characterization and modeling of the peripheral cardiac conduction system. IEEE Transactions on Medical Imaging **32**(1), 45–55 (2013).
27. J. Keener and J. Sneyd.: Mathematical physiology. Springer, (1998).
28. J. Sundnes, G. T. Lines, X. Cai, B. F. Nielsen, K. A. Mardal, and A. Tveito.: Computing the electrical activity in the heart. Springer Science & Business Media, (2007).
29. K. Ten Tusscher and A. Panfilov.: Modelling of the ventricular conduction system. Progress in Biophysics and Molecular Biology **96**(1), 152–170 (2008).
30. J. T. Bigger and W. J. Mandel.: Effect of lidocaine on conduction in canine Purkinje fibers and at the ventricular-muscle-Purkinje fiber junction. Journal of Pharmacology and Experimental Therapeutics **172**(2), 239–254 (1970).
31. D. G. Kassebaum and A. R. Van Dyke.: Electrophysiological effects of isoproterenol on Purkinje fibers of the heart. Circulation Research **19**(5), 940–946 (1966).

ICCS Camera Ready Version 2019
To cite this paper please use the final published version:
DOI: 10.1007/978-3-030-22744-9_6